

Semi-Empirical Theory of the Nuclear Energy Surface*

EUGENE FEENBERG

Washington University, Saint Louis, Missouri

The semi-empirical theory of the nuclear energy surface as a sum of volume, surface, symmetry, Coulomb, and expansion terms has been subjected to critical revision. A quantitative correlation appears to exist between the windings of the mass valley in the $N-Z$, A plane and irregularities (plateaus) in the packing fraction curve. The theoretical Pf curve and the various energy parameters are fixed within narrow limits by the mass differences of odd isobars ($N-Z = \pm 1$) independent, within wide limits, of the value assigned to the compressibility coefficient. Two procedures (the analysis of nuclear fission, the fitting of the theoretical Pf curve) yield independent values for the ratio surface energy/Coulomb energy. These values differ, presumably because the first involves the size of the real nucleus, whereas the second, through the assumption $R = r_v A^{1/3}$, refers to a uniform state of nuclear matter as it would be in the absence of internal pressures tending to produce expansion. A reasonable value of the compressibility coefficient, consistent with estimates based on the virial theorem, suffices to account for the computed 10 percent difference. A general proof is found for Wigner's rule that isotopic numbers $N-Z = 2n-1$ and $N-Z = 2n$ first occur at nearly the same values of A .

(A) INTRODUCTION

THESE notes are concerned with the critical discussion and evaluation of a simple semi-empirical energy formula based on the concept of a nearly constant average density of nuclear matter throughout the range of known nuclear species. The essential structure and properties of the formula are well known¹⁻³ but no entirely adequate treatment in the light of present knowledge is available. Adopting the simplest

* The research described in this paper was supported in part by contract N60RI-117, U. S. Navy Department.

¹ C. F. v. Weizsacker, *Zeits. f. Physik* **96**, 431 (1935).

² H. A. Bethe and R. F. Bacher, *Rev. Mod. Phys.* **8**, 82 (1936).

³ P. Jordan, *Ergeb. d. exakt. Naturwiss.* (1937).

possible analytical representation we write

$$E(N, Z) = E_v + E_s + E_r + E_c - (E_s' + E_r' + E_c)^2 / 2E_v'' \quad (1)$$

for the normal state energy of a nucleus containing N neutrons and Z protons. Here

$$\begin{aligned} E_v &= -u_v A, \\ E_s &= u_s A^{2/3}, \\ E_r &= u_r \frac{(N-Z)^2}{A}, \\ E_c &= 4u_c \frac{Z(Z-1)}{A^{1/3}}. \end{aligned} \quad (2)$$

All dependence on the even-odd character of N and Z may properly be ignored in the preliminary survey. The modifications required to adapt Eqs. (1) and (2) to the observed even-odd dependence are reserved for discussion in section (F).

In Eq. (1) the first term may be interpreted as volume energy in view of the proportionality of volume and total number of particles (an alternative statement of the basic assumption). The surface area varies as $A^{2/3}$, permitting the identification of the second terms in Eq. (1) as surface energy. Since the third term is a homogeneous function of the first degree in N and Z , it might properly be grouped with the volume energy. However, the designation symmetry (or isotopic spin) energy proves convenient. A similar term can be derived from the crude nuclear model of non-interacting particles in a potential well. The fourth term is the electrostatic or coulomb energy. The electrostatic energy of a uniformly charged sphere of radius R_v and total charge Ze has the value $3(Ze)^2/5R_v$. From this relation and

$$R_v = r_v A^{1/3}, \quad (3)$$

we infer

$$u_c = 3e^2/20r_v. \quad (4)$$

In particular, for $r_v = r_0 \equiv 1.47 \times 10^{-13}$ cm, $u_c = 0.157$ millimass units, the value required by the empirical mass differences of odd isobars with $N - Z = \pm 1$ under the assumption that nuclear matter is incompressible.⁴⁻⁷

At this point there is need for a critical examination of the basic assumption. It seems plausible that the assumption should apply, not to actual nuclei, but to hypothetical nuclear systems in which

(a) the electrostatic interaction between protons is absent.

(b) the internal pressure associated with the surface energy is negligible (essentially imposes a lower limit on the mass number A).

(c) N and Z are even integers and $N = Z$.

Conditions (a) and (c) define a neutral four-group type of nuclear matter.

Under the assumed conditions the energy has the form $E_v + E_s$, and the surface energy does not enter into the determination of the equilibrium radius R_v . Turning now to actual nuclei, E_v , E_s , E_τ , and E_c are all evaluated at the particle density defined by Eq. (3). The last term in the right-hand member of Eq. (1) arises from the change in volume of the nucleus under the internal pressure produced by the electrostatic force and by the deficiency in binding energy associated with E_s and E_τ . The "compressibility" coefficient E_v'' is the second derivative of the volume energy with respect to a uniform scale factor. A general argument (essentially an application of the virial theorem) leads to the result⁸

$$E_v'' \sim 2T_v k_v, \quad (5)$$

in which T_v is the total kinetic energy associated with E_v . Some uncertainty attaches to the coefficient k_v , but it seems likely to fall in the neighborhood of 2 to 3. Adopting a reasonable

estimate for T_v , Eq. (5) yields

$$E_v'' \sim (50 \text{ to } 100)A \text{ mMU}. \quad (6)$$

The rates of change of E_s and E_τ with respect to a linear scale factor are denoted by E_s' and E_τ' . These derivatives are proportional to E_s and E_τ , respectively; hence

$$\begin{aligned} E_s' &= k_s E_s, \\ E_\tau' &= k_\tau E_\tau. \end{aligned} \quad (7)$$

A more complete discussion of Eqs. (5)–(7) appears in the following section.

The packing fraction⁹ provides a convenient representation of the experimental material. With energy expressed in mMU and $n = 1.00892$, $H = 1.00813$, the packing fraction is related to the energy per particle in the following simple manner:

$$\begin{aligned} Pf \times 10^3 &\equiv (M - A/A)10^3 \\ &= 8.53 + 0.40(N - Z/A) + E/A. \end{aligned} \quad (8)$$

Experimental packing fraction curves have been plotted by Dempster¹⁰ and by Hahn, Fluegge, and Mattauch.¹¹ A considerable element of interpretation is involved in the experimental curves, since a number of points are derived from packing fraction differences alone. There are features of Dempster's curve which find no counterpart in the theory provided by Eq. (1). Especially striking is the flat plateau between W and Pb required by the experimental fact that the slope of the packing fraction curve in the mass range 90–105 is double that in the range 180–210. One might attempt to correlate the plateau with the development of a two-phase system; an inner region consisting mostly of neutrons and an outer region in which there is a trend toward approximately equal numbers of neutrons and protons. The incipient stages of such a development would be marked by an additional negative term in Eq. (1) associated with the variation in neutron and proton densities within the nucleus arising from the electrostatic repulsion of the protons. Crude estimates of these effects suggest that they are not large in actual nuclei.^{12,13}

⁹ F. W. Aston, *Mass Spectra and Isotopes* (Edward Arnold and Company, London, England, 1942).

¹⁰ A. J. Dempster, *Phys. Rev.* **53**, 869 (1938).

¹¹ O. Hahn, S. Fluegge, and J. Mattauch, *Physik. Zeits.* **41**, 1 (1940).

¹² E. Feenberg, *Phys. Rev.* **59**, 593 (1941).

¹³ E. Wigner, Bicentennial Symposium, University of Pennsylvania (1940).

⁴ E. Wigner, *Phys. Rev.* **51**, 947 (1937).

⁵ W. Barkas, *Phys. Rev.* **55**, 694 (1939).

⁶ D. R. Elliot and L. D. P. King, *Phys. Rev.* **60**, 489 (1941).

⁷ E. Feenberg and G. Goertzel, *Phys. Rev.* **70**, 597 (1946).

⁸ E. Feenberg, *Phys. Rev.* **59**, 149 (1941). Detailed calculations of the compressibility coefficient have been made by K. Nakabayasi, *Zeits. f. Physik* **97**, 211 (1935); H. Bethe and R. F. Bacher, *Rev. Mod. Phys.* **8**, 82 (1936); R. D. Present, *Phys. Rev.* **60**, 28 (1941). These calculations involve the application of the statistical approximation to exchange type force models. The results conform to Eq. (6). Present also obtains estimates for E_s' and E_τ' .

A second representation considered by Dempster places a point of inflexion (or possibly a plateau) near $A = 105$. The experimental points in this region are compatible with the existence of a nearly horizontal plateau extending over the range $108 \leq A \leq 124$. It is then possible to eliminate the plateau between W and Pb by considerably increasing the slope in the range $90 \leq A \leq 105$. Dempster's curve and also the second possibility both appear in Fig. 1. Evidently the danger of widespread α -instability below $A = 180$ is reduced by the shift of the plateau from the range 180–210 to 108–124. As shown in Section (E), the second representation can be interpreted quantitatively within the framework of Eq. (1). The plateau in the mass number range 108–124 is a natural and unforced consequence of the empirical dependence of u_τ on mass number.

Hahn, Fluegge, and Mattauch utilize the freedom available in interpreting the data to minimize the possibility of α -particle emission below

the heavy radioactive elements. They obtain essentially the second possibility discussed above with a clearly defined plateau in the range 108–124.

In the preliminary survey it seems desirable to ignore the detailed structure of the packing fraction curve and to seek for the optimum quantitative representation of selected groups of experimental data. These are:

(a) Smoothing out local oscillations, the isotopic number $N-Z$ is a fairly regular and simple function of the mass number.

(b) The packing fraction attains the minimum value -0.74 mMU in the general neighborhood of $A = 60$.

(c) The packing fraction vanishes at mass numbers 16 and 173.

(d) The energy difference between odd isobars with $N-Z = \pm 1$ follows closely the formula

$$\Delta E_o = 0.628(A-1)/A^{\frac{1}{2}} \text{ mMU } (A \geq 15).$$

With (d) always satisfied, we find that u_τ and u_o are practically independent of the compressibility coefficient. Numerical relations derived

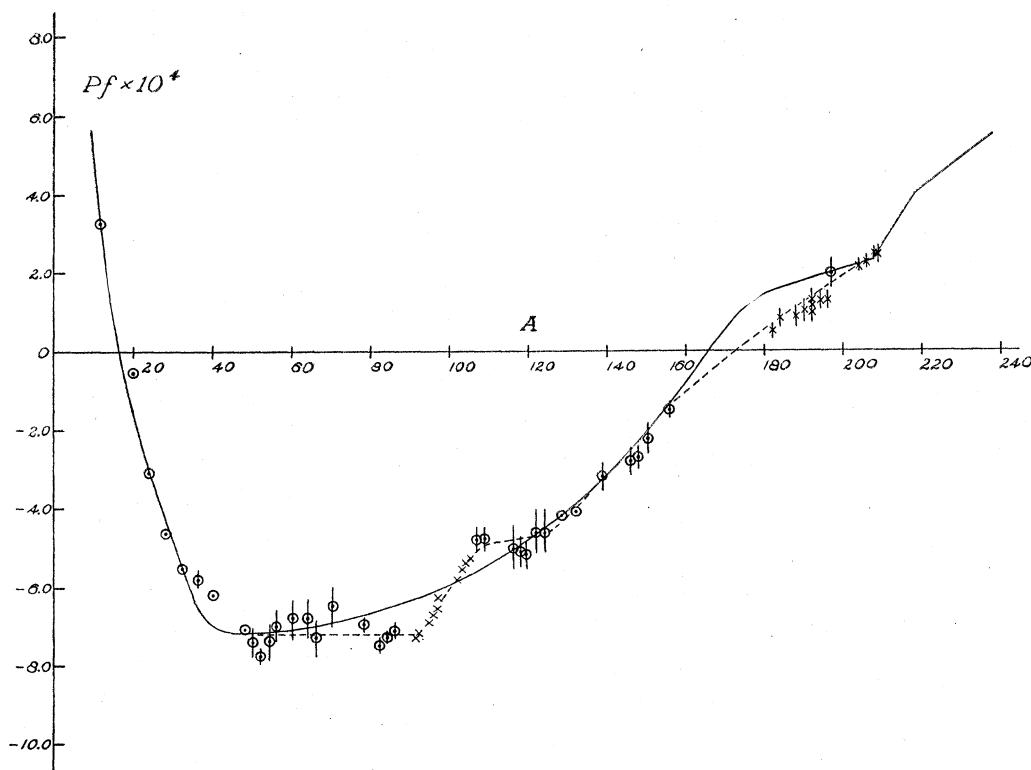


FIG. 1. Experimental packing fraction curves. Solid curve—Dempster (a); dashed curve—Dempster (b); ϕ —experimental points (Hahn, Fluegge, and Mattauch); x —estimated from Dempster's packing fraction differences.

from (a), (b), (c), (d) and Eqs. (1) and (2) are collected in Table V. Following the preliminary survey the discussion turns to problems involving the irregularities of the packing fraction curve and the even-odd properties of nuclear systems.

(B) THE COMPRESSIBILITY COEFFICIENT
OF NUCLEAR MATTER AND
RELATED QUANTITIES

Let H_a represent the nuclear Hamiltonian with omission of the Coulomb interaction. The equation

$$H_a \psi_a = E_a \psi_a \quad (9)$$

determines the normal state eigenfunction $\psi_a(x_1, y_1, \dots)$ and eigenvalue $E_a(N, Z)$ of a nuclear model in which there is no Coulomb force between protons. The eigenvalue $E(N, Z)$ and radius R of an actual nucleus may be computed to a sufficient degree of approximation from the expectation value of the total Hamiltonian using as wave function $\psi_a(\lambda x_1, \lambda y_1, \dots)$ with λ a scale factor to be determined by minimizing E . Thus⁸

$$E(N, Z, \lambda)$$

$$= \frac{\int \dots \int \psi_a^*(\lambda x, \dots) H_a \psi_a(\lambda x, \dots) dv}{\int \dots \int [\psi_a(\lambda x, \dots)]^2 dv} + \lambda E_c \quad (10)$$

$$= E_a(N, Z, \lambda) + \lambda E_c.$$

To express $E_a(N, Z, \lambda)$ as a sum of volume, surface, and symmetry energies consider a system containing A' particles with $A' \gg A$ and $Z' = N' = \frac{1}{2}A'$. Then

$$E_v(A, \lambda) = \lim_{A' \rightarrow \infty} \frac{A}{A'} E_a\left(\frac{A'}{2}, \frac{A'}{2}, \lambda\right),$$

$$E_s(A, \lambda) = \lim_{A' \rightarrow \infty} \left[E_a\left(\frac{A}{2}, \frac{A}{2}, \lambda\right) - \frac{A}{A'} E_a\left(\frac{A'}{2}, \frac{A'}{2}, \lambda\right) \right], \quad (11)$$

$$E_r(N, Z, \lambda) = E_a(N, Z, \lambda) - E_a\left(\frac{A}{2}, \frac{A}{2}, \lambda\right)$$

and

$$E(N, Z, \lambda) = E_v(A, \lambda) + E_s(A, \lambda) + E_r(N, Z, \lambda) + \lambda E_c(A, Z). \quad (12)$$

It is evident from the definition of E_v that

$$E_v' \equiv \left(\frac{\partial E_v}{\partial \lambda} \right)_{\lambda=1} = 0. \quad (13)$$

Consequently,

$$E(N, Z, \lambda) \cong E_v(A, 1) + E_s(A, 1) + E_r(N, Z, 1) + E_c(A, Z) + (\lambda - 1) \times [E_s'(A, 1) + E_r'(N, Z, 1) + E_c(A, Z)] + \frac{1}{2}(\lambda - 1)^2 E_v''(A, 1). \quad (14)$$

From the condition for a minimum there follows

$$\lambda \equiv R_v/R = 1 - (E_s' + E_r' + E_c)/E_v'',$$

$$E(N, Z, \lambda) = E(N, Z, 1) - (E_s' + E_r' + E_c)^2 / 2E_v''. \quad (15)$$

To obtain an order of magnitude estimate of the compressibility coefficient E_v'' it is convenient to express $E_v(A, \lambda)$ as a sum of potential and kinetic energy matrix elements, i.e.,

$$E_v(A, \lambda) = \lambda^2 T_v - U_v(\lambda). \quad (16)$$

The coefficient λ^2 multiplying T_v is a consequence of the fact that the kinetic energy operator transforms as a homogeneous function of degree -2 in the space coordinates under a change of scale. Equation (13) now yields

$$U_v'(1) = 2T_v. \quad (17)$$

The calculations of Section (D) determine E_v to have the value $-15A$ mMU independent of the magnitude assigned to the "expansion" energy, subject to the condition that the mass difference of isobaric odd nuclei with $N - Z = \pm 1$ is given correctly by the theory. The statistical model (Section (H)) yields $T_v \sim 15A(r_0/r_v)^2$ mMU. Thus

$$U_v(1) \sim T_v \left[1 + \left(\frac{r_v}{r_0} \right)^2 \right]. \quad (18)$$

Results are stated for three analytical forms of

the potential matrix element:

$$\begin{array}{ccc}
 U_v(\lambda) & a & k_v \\
 B \exp(-a/\lambda) & \frac{2}{(1+(r_v/r_0)^2)} & \frac{1+3(r_v/r_0)^2}{1+(r_v/r_0)^2} \\
 B \exp[-(a/\lambda)^2] & \frac{1}{(1+(r_v/r_0)^2)^{\frac{3}{2}}} & \frac{1+2(r_v/r_0)^2}{2(1+(r_v/r_0)^2)} \\
 B\lambda^3/(\lambda^2+a^2)^{\frac{3}{2}} & \left(\frac{2}{1+3(r_v/r_0)^2}\right)^{\frac{3}{2}} & \frac{2}{3} \frac{1+6(r_v/r_0)^2}{1+(r_v/r_0)^2}
 \end{array} \quad (19)$$

Two other problems of general interest can be treated conveniently in this context. First it is plausible that the nuclear radius should depend slightly on the state of excitation. To obtain a semi-quantitative relation between radius and excitation energy consider the equation

$$\tilde{E}_v(\lambda) = (1 + \delta_1)\lambda^2 T_v - (1 - \delta_2)U_v(\lambda) \quad (20)$$

in which δ_1 and δ_2 represent the relative increase in kinetic energy and decrease in potential energy, respectively, of the excited state. The minimum value of \tilde{E}_v occurs at

$$\lambda = 1 - (\delta_1 + \delta_2)/k_v \quad (21)$$

or

$$\tilde{R}/R_v = 1 + (\delta_1 + \delta_2)/k_v,$$

and the excitation energy is simply

$$\Delta E_{\text{exc}} = \delta_1 T_v + \delta_2 U_v \sim \frac{1}{2}(\delta_1 + 2\delta_2)U_v. \quad (22)$$

Equations (21) and (22) together yield

$$\frac{\Delta E_{\text{exc}}}{k_v U_v} \cong \frac{\tilde{R} - R_v}{R_v} \cong \frac{2\Delta E_{\text{exc}}}{k_v U_v}. \quad (23)$$

For a numerical example suppose N_e^{20} is excited by the absorption of a slow meson. Then $\Delta E_{\text{exc}} \sim 100$ mMU and, with $k_v U_v \sim 1200$ mMU, the expansion lies between 8 percent and 16 percent of the normal state radius. This expansion is large enough to reduce materially the potential barrier involved in the emission of low energy protons. Another effect facilitating the emission of low energy protons has been discussed by Bagge.¹⁴ The excitation of "surface" vibrations produces an increase in the mean square radius and thus a decrease in the effective Coulomb

barrier. The two effects are comparable in magnitude and doubtless both occur in actual nuclear systems.

The second problem concerns the stability of the spherical shape in heavy nuclei. All available discussions are based on the assumption that nuclear matter is incompressible. However, a finite value of the compressibility coefficient, consistent with Eq. (6), appears necessary to bring about concordance between results obtained from

- (a) the analysis of the packing fraction curve (Section (D)) and
- (b) the analysis of the fission process.¹⁵

Suppose that E_a and the Coulomb energy are expressed as functions of two parameters, λ a scale factor, and μ a shape factor. These are defined conveniently by the equation

$$x^2 + y^2 + \left(\frac{z}{\mu}\right)^2 = R_v^2/\lambda^2 \mu^3, \quad (24)$$

representing the surface of the nucleus under the combined action of a uniform change of scale and an ellipsoidal distortion. In terms of λ and μ

$$E(\lambda, \mu) = E_v(\lambda) + E_s(\lambda, \mu) + E_r(\lambda) + \lambda E_c(\mu). \quad (25)$$

Equation (25) can be studied conveniently by expanding $E(\lambda, \mu)$ in a double power series about the point $\lambda = \mu = 1$:

$$\begin{aligned}
 E(\lambda, \mu) = & E(1, 1) + (\lambda - 1)[E_s' + E_r' + E_c] \\
 & + \frac{1}{2}(\lambda - 1)^2 E_v'' + \frac{1}{2}(\mu - 1)^2 \\
 & \times (E_{s\mu\mu} + (\lambda - 1)E_{s\mu\mu}' + \lambda E_{c\mu\mu}) + \dots
 \end{aligned} \quad (26)$$

The notation of primes to indicate derivatives

¹⁵ N. Bohr and J. A. Wheeler, Phys. Rev. **56**, 426 (1939).

¹⁴ E. Bagge, Ann. d. Physik **33**, 27 (1938).

TABLE I. $[k_s u_s A^{\frac{1}{3}} + u_c (A-1)^2 / A^{\frac{1}{3}}] / 50A$.

$A \backslash k_s$	-1.00	-0.50	-0.25	0.00	0.25	0.50	1.00	1.50
15	-0.093	-0.038	-0.011	0.017	0.044	0.071	0.126	0.180
23	-0.072	-0.024	-0.001	0.023	0.047	0.071	0.118	0.165
31	-0.057	-0.014	0.007	0.029	0.051	0.072	0.115	0.158

with respect to λ is continued, and derivatives with respect to μ are denoted by the subscript μ . All derivatives are evaluated at $\lambda = \mu = 1$.

For the purpose of studying the stability of the spherical shape $\mu - 1$ is treated as an arbitrarily small quantity; consequently the equilibrium value of λ is identical with that already computed (Eq. 15). The spherical shape is stable against small ellipsoidal deformations if the coefficient of $(\mu - 1)^2$ is positive. According to the elementary theory of fission¹⁶⁻¹⁹

$$E_{s\mu\mu} = \frac{16}{45} E_s, \quad E_{c\mu\mu} = -\frac{8}{45} E_c. \quad (27)$$

Thus the stability condition can be expressed in the form

$$\frac{2E_s(\lambda, 1)}{\lambda E_c(1)} > 1 \quad (28)$$

or, explicitly,

$$\frac{u_s}{u_c} > \frac{2Z(Z-1)}{A} \left[1 - (1-k_s) \frac{k_\tau E_\tau}{E_v''} - \frac{E_c}{2E_v''} (2+k_s)(1-k_s) \right]. \quad (29)$$

The factor in square brackets is new. In the absence of this factor Bohr and Wheeler find that u_s/u_c has the value

$$\left(\frac{u_s}{u_c} \right)_{BW} = \frac{2 \times 92 \times 91}{239} \frac{1}{0.74} = 94.7. \quad (30)$$

TABLE II. u_c and r_v as functions of k_s .

k_s	E_v'' (mMU)	u_c (mMU)	$r_v \cdot 10^{13}$ (cm)
0.00	50A	0.161	1.44
0.50	50A	0.169	1.37
1.00	50A	0.178	1.30
0.50	30A	0.178	1.30

¹⁶ E. Feenberg, Phys. Rev. **55**, 504 (1939).

¹⁷ C. F. v. Weizsacker, Naturwiss. **27**, 133 (1939).

¹⁸ J. Frenkel, Phys. Rev. **55**, 987 (1939).

¹⁹ M. S. Plessett, Am. J. Phys. **9**, 1 (1941).

The number 0.74 appearing in Eq. (30) is a measure of the potential barrier opposing the spontaneous fission of ${}_{92}\text{U}^{239}$. Provisionally, the same number may be combined with Eq. (28) to produce the equality

$$\frac{u_s}{u_c} = 94.7 \left[1 - (1-k_s) \frac{k_\tau E_\tau}{E_v''} - (1-k_s)(1.48+k_s) \frac{E_c}{1.48E_v''} \right]. \quad (31)$$

Here the square bracket is evaluated at $A = 239$, $Z = 92$.

Reliable theoretical estimates of k_s and k_τ are lacking. However, k_τ can hardly be negative considering that the kinetic and potential energies both increase with decreasing radius (increasing λ). It is therefore plausible that the additional kinetic energy and the deficiency of potential energy associated with $N - Z \neq 0$ should also increase with decreasing radius. In view of the fact that the ratio E_τ/E_c is small, no attempt will be made to determine k_τ from the empirical data.

To determine the sign of k_s we observe that the particle density at the center of very light nuclei may reasonably be expected to increase with increasing mass number under conditions (a) and (c) of the introduction. An equivalent statement is contained in Eq. (15) provided that $E_s' > 0$. Thus k_s should be positive.

Upper and lower limits on k_s can be derived from the combination of empirical data on Coulomb energy differences in odd isobars with the hypothesis that Eqs. (1) and (2) are valid down to mass number 15. The theoretical energy difference is

$$\Delta E(N-Z = \pm 1) = \frac{4u_c(A-1)}{A^{\frac{1}{3}}} \times \left[1 - \frac{k_s E_s + k_\tau E_\tau + u_c (A-1)^2 / A^{\frac{1}{3}}}{E_v''} \right], \quad (32)$$

while the empirical differences are represented adequately by the first factor only (omitting the factor in square brackets) with $u_c = 0.157$ mMU. Considering the accuracy and number of the experimental measurements, the latter factor

cannot vary by more than 2 percent in the range $15 \leq A \leq 31$. Numerical results for

$$\begin{aligned} E_v'' &= 50A \text{ mMU}, \\ u_c &= 0.157 \text{ mMU}, \\ u_s &= 13.5 \text{ mMU} \end{aligned} \quad (33)$$

are shown in Table I. The variation in the vertical columns is less than 0.02 on the interval $-0.25 \leq k_s \leq 1.00$ and practically vanishes at $k_s = 0.50$. Evidently the optimum value of u_c depends on k_s in accordance with the relation

$$u_c \left\langle 1 - \frac{k_s E_s + k_\tau E_\tau + u_c (A-1)^2 / A^{\frac{1}{3}}}{E_v''} \right\rangle = 0.157 \text{ m}\mu, \quad (34)$$

the symbol $\langle \rangle$ denoting a mean value on the interval $15 \leq A \leq 31$. Equation (34) states simply that the actual radii of real nuclear systems conform closely to the formula $1.47 \times 10^{-13} A^{\frac{1}{3}}$ cm. The numerical solution of Eq. (34) appears in Table II.

In the event that k_s is negligible, the condition $E_v'' > 30A$ mMU is required to keep the variation in the square bracket factor of Eq. (32) within the permitted range of 2 percent. On the other hand, the preceding analysis places no useful restriction on the compressibility coefficient if $k_s \sim 0.5$. The inclusion of a symmetry energy term $k_\tau E_\tau$ with reasonable restrictions on k_τ does not materially alter the numbers in Tables I and II.

(C) THE NEUTRON EXCESS IN STABLE NUCLEI

For fixed A the mass and packing fraction attain minimum values when Z takes on the integral value closest to

$$Z_A = \frac{1}{2} \frac{\beta A}{1 + \gamma A^{\frac{2}{3}}}, \quad \gamma = u_c / u_\tau \quad (35)$$

with

$$\beta = 1 + \gamma \left[\frac{2}{u_c} + \frac{1}{A^{1/3}} + \frac{1 - k_\tau}{E_v''} \left(\frac{k_s u_s A^{4/3}}{1 + \gamma A^{2/3}} + \frac{u_c A^{7/3} (1 + k_\tau \gamma A^{2/3})}{(1 + \gamma A^{2/3})^3} \right) \right]. \quad (36)$$

The notation

$$\begin{aligned} X_1 &= (1 + \gamma A^{\frac{2}{3}}) \left(\frac{1}{A} + \frac{0.2}{u_c A^{\frac{1}{3}}} \right), \\ X_2 &= \frac{1 - k_\tau}{E_v''} \left[k_s u_s A^{2/3} + \frac{u_c A^{5/3} (1 + k_\tau \gamma A^{2/3})}{(1 + \gamma A^{2/3})^2} \right] \end{aligned} \quad (37)$$

proves helpful in transforming Eq. (35) into the more useful form

$$2\gamma = \frac{A - 2Z_A}{A^{\frac{1}{3}} Z_A} [1 - X_1 - X_2]^{-1}. \quad (38)$$

The left-hand member of Eq. (38) is nominally a constant. However, the hypothesis that the symmetry energy is a homogeneous function of the first degree in N and Z is possibly too special. The presence in the symmetry energy of a term

TABLE III.

Z	$\frac{A-2Z}{A^{2/3}Z}$	Z	$\frac{A-2Z}{A^{2/3}Z}$
92	0.0153	53	0.0157
91	0.0143	52	0.0179
90	0.0153	51	0.0159
89	0.0148	50	0.0155
88	0.0153	49	0.0146
87	—	48	0.0147
86	0.0158	47	0.0131
85	—	46	0.0141
84	0.0141	45	0.0131
83	0.0147	44	0.0138
82	0.0151	43	—
81	0.0151	42	0.0136
80	0.0148	41	0.0131
79	0.0146	40	0.0140
78	0.0149	39	0.0142
77	0.0149	38	0.0156
76	0.0152	37	0.0160
75	0.0148	36	0.0173
74	0.0150	35	0.0154
73	0.0150	34	0.0176
72	0.0151	33	0.0153
71	0.0149	32	0.0155
70	0.0153	31	0.0148
69	0.0147	30	0.0111
68	0.0151	29	0.0122
67	0.0154	28	0.0065
66	0.0156	27	0.0122
65	0.0152	26	0.0103
64	0.0156	25	0.0138
63	0.0145	24	0.0121
62	0.0150	23	0.0158
61	—	22	0.0135
60	0.0148	21	0.0113
59	0.0144	20	0.0005
58	0.0155	19	0.0052
57	0.0163	18	0.0188
56	0.0170	17	0.0080
55	0.0160		
54	0.0167		

of degree two-thirds would require

$$u_\tau = u_{\tau v} + u_{\tau s}/A^{\frac{1}{3}},$$

$$\gamma = \frac{\gamma_v}{1 + \frac{u_{\tau s}}{u_{\tau v} A^{\frac{1}{3}}}}. \quad (39)$$

Regarding numerical values two points can be made: (1) the model of free particles in a potential well of infinite depth²⁰ yields $u_{\tau s}/u_{\tau v} = 0.4$. As the depth of the well is reduced, the ratio decreases and attains a small negative value (~ -0.1) for a reasonable depth (~ 30 mMU). (2) In actual nuclei the surface energy may be expected to decrease with increasing isotopic number more or less paralleling the behavior of the volume energy. The second point suggests a small negative value for $u_{\tau s}$.

In evaluating the right-hand member of Eq. (38) the proper value of A to associate with a given Z is generally not known accurately, but a suitable approximation is provided by the mean mass number¹¹ since there appears to be a close correlation between abundance and stability.

The functions X_1 and X_2 occur in Eq. (38) because of three small, but physically real, effects. These are

- (xa) the neutron-hydrogen mass difference,
- (xb) the linear term in Z in the Coulomb energy,
- (xc) the "expansion" energy associated with the finite value of the compressibility coefficient.

Since both functions involve γ , a preliminary estimate of γ must be secured before the right-hand member of Eq. (38) can be evaluated. Table III lists the quantity

$$X_0 \equiv \frac{A - 2Z_A}{A^{\frac{1}{3}} Z_A}$$

TABLE IV. Evaluation of X_1 and X_2 .

A	$k_s = k_\tau = 0$			$k_s = 0.5, k_\tau = 0$	
	X_1	X_2	$X_1 + X_2$	X_2	$X_1 + X_2$
64	0.108	0.039	0.147	0.073	0.181
125	0.071	0.054	0.125	0.081	0.152
216	0.052	0.067	0.119	0.089	0.141
343	0.041	0.077	0.118	0.096	0.137

²⁰ E. Feenberg, Phys. Rev. 60, 204 (1941).

as a function of atomic number with A replaced by the mean mass number.

In the range $Z \geq 31$, X_0 experiences large fluctuations, but there is no sign of a trend. A sharp break occurs at $Z = 30$. Consider first the upper range $58 \leq Z \leq 92$. Here the mean value is 0.0150 and the fluctuations are small and quite random. It is interesting that of the ten deviations from the mean exceeding ± 0.0003 , eight occur for elements containing substantially only one isotope. Evidently the mean mass number of an element composed of several relatively abundant isotopes generally lies very close to the smooth curve defined by A as a function of Z_A . On the lower range $31 \leq Z \leq 57$ the mean value is 0.0152, and the deviations from the mean are large and oscillatory in a systematic way. The present theory can be made to fit the behavior of X_0 on the upper range but cannot account for the oscillations on the lower range. Possibly these may be interpreted in terms of shell structure. Disregarding the oscillations, $X_0 = 0.0150$ holds well enough on the average down to $Z = 31$.

Suppose that X_2 is omitted from the right-hand member of Eq. (38), X_0 replaced by 0.0150, and γ and u_c given the provisional values 0.0080 and 0.157, respectively, in evaluating X_1 . It is found that the function equated to 2γ is not constant but exhibits a monotonic variation in the range $Z \geq 31$, amounting to 6 percent of the mean value. On the upper range the variation is 2 percent, somewhat greater than any possible systematic trend in X_0 . Assuming that all or part of this variation is balanced by the symmetry dependence of the surface energy, we get

$$0 < -(u_{\tau s}/u_{\tau v}) \leq 0.6. \quad (40)$$

The effect of X_2 on the right-hand member of Eq. (38) is apparent from Table IV, based on the provisional values $\gamma = 0.0085$, $u_c = 0.157$ mMU, and $E_v'' = 50A$ mMU.

Now the monotonic variation in the upper range of the function equated to 2γ is reduced to 0.7 percent ($k_s = 0$) or 1.3 percent ($k_s = 0.5$). The upper limit in Eq. (40) is correspondingly reduced to 0.2 ($k_s = 0$) or 0.4 ($k_s = 0.5$). The best constant value for γ appears to be 0.0085 ($k_s = 0$) and 0.0088 ($k_s = 0.5$). If u_c is taken from Table II these values are not appreciably altered. For any

choice of k_s a finite positive value for k_r reduces X_2 and the mean value of γ and permits a larger upper bound on $-u_{rs}/u_{rv}$.

(D) THE PACKING FRACTION CURVE IN THE REGION OF STABLE NUCLEI

It is evident from Eqs. (1) and (8) that the packing fraction formula can be expressed as a fourth-degree polynomial in $Z-Z_A$. The third and fourth degree terms may be omitted without appreciable loss of accuracy leaving the simple quadratic polynomial

$$Pf \times 10^3 = (Pf \times 10^3)_{Z_A} + \frac{1}{2} \left(\frac{\partial^2}{\partial Z^2} Pf \times 10^3 \right)_{Z_A} (Z-Z_A)^2. \quad (41)$$

In Eq. (40)

$$\begin{aligned} & \frac{1}{2} \left(\frac{\partial^2}{\partial Z^2} Pf_A 10^3 \right)_{Z_A} \\ &= \frac{4u_c}{\gamma A^2} \left[1 + \gamma A^{2/3} - \frac{1}{E_v''} \left\{ (k_r + \gamma A^{2/3}) \right. \right. \\ & \times \left(k_s u_s A^{2/3} + \frac{u_c A^{5/3} (1 + k_r \gamma A^{2/3})}{(1 + \gamma A^{2/3})^2} \right) \\ & \left. \left. + \frac{2u_c \gamma (1 - k_r)^2 A^{7/3}}{(1 + \gamma A^{2/3})^2} \right\} \right]. \quad (42) \end{aligned}$$

The constant term is best evaluated by grouping together linear and quadratic terms in Z except those implicit in the expansion terms. With the notation

$$Z_A' = Z_A \quad \text{for} \quad E_v'' = \infty$$

the result of the grouping procedure is

$$\begin{aligned} Pf \times 10^3 &= 8.53 - u_v + \frac{u_s}{A^{1/2}} \\ &+ u_c A^{3/2} \frac{1 + (0.4\gamma/u_c) - (2/A)}{(1 + \gamma A^{3/2})} \\ &+ \frac{4u_c}{\gamma A^2} (1 + \gamma A^{3/2}) (Z - Z_A')^2 \\ &- \frac{1}{2AE_v''} \left\{ k_s u_s A^{3/2} + k_r u_r \frac{(A - 2Z)^2}{A} \right. \\ & \left. + \frac{4u_c}{A^{1/2}} Z(Z - 1) \right\}. \quad (43) \end{aligned}$$

The factor $1 + (0.4\gamma/u_c) - (2/A)$ is not exact; however the neglected terms total less than 0.002 at $A = 64$ and decrease as A increases. To a sufficient degree of accuracy

$$\begin{aligned} (Pf \times 10^3)_{Z_A} &= 8.53 - u_v + \frac{u_s}{A^{1/2}} \\ &+ u_c A^{3/2} \frac{1 + (0.4\gamma/u_c) - (2/A)}{1 + \gamma A^{3/2}} \\ &- \frac{u_c^2 A^{3/2}}{2E_v''} \left[\frac{u_s}{u_c} + \frac{A(1 + k_r \gamma A^{3/2})}{(1 + \gamma A^{3/2})^2} \right]^2. \quad (44) \end{aligned}$$

The symmetry energy utilized in the derivation of Eq. (44) fails to account for the sharp break in X_0 below $Z = 31$ (Table III). Consequently the range of validity of Eq. (44) presumably does not extend down to the minimum of the packing fraction curve. Below $Z = 20$, Eq. (44) should be replaced by

$$\begin{aligned} (Pf \times 10^3)_{Z=A/2} &= 8.53 - u_v + \frac{u_s}{A^{1/2}} + u_c A^{3/2} (1 - 2/A) \\ &- \frac{u_c^2 A^{3/2}}{2E_v''} \left[\frac{u_s}{u_c} + A(1 - 2/A) \right]^2. \quad (45) \end{aligned}$$

in the approximation which ignores the even-odd properties of N and Z .

Equations (44) and (45) are now subjected to the condition $Pf = 0$ at $A = 16$ and 173. It is desirable to proceed as far as possible without fixing the numerical value of u_c . However, where u_c is involved in a small correction term we use the following table:

k_s	u_c	$\frac{0.4\gamma}{u_c}$	$\frac{u_c A}{2E_v''}$	$\frac{u_s}{u_c}$
0.0	0.161	0.021	0.0016	86
0.5	0.169	0.021	0.0017	86

The reduction of Eqs. (44) and (45) to numerical form yields, for $k_s = k_r = 0$,

$$\begin{aligned} 8.53 - u_v + 0.3969u_s + (5.55 - 0.05)u_c &= 0, \\ 8.53 - u_v + 0.1795u_s + (24.79 - 0.59)u_c &= 0 \quad (46) \end{aligned}$$

and, for $k_s=0.5$, $k_r=0$,

$$\begin{aligned} 8.53 - u_v + 0.3969u_s + (5.55 - 0.87)u_c &= 0, \\ 8.53 - u_v + 0.1795u_s + (24.60 - 1.25)u_c &= 0. \end{aligned} \quad (47)$$

The contributions from the first-order Coulomb energy and the "expansion" energy are listed separately to show the order of magnitude of the latter term. Numerical results computed from Eqs. (46) and (47) are listed in the first two rows of Table V. For comparison results obtained from the conditions

$$Pf=0, \quad A=16 \text{ and } 173; \quad E_v''=30A \text{ mMU}, \\ k_s=0.5, \quad u_c=0.178$$

$$Pf=0, \quad A=16 \text{ and } 173; \quad E_v''=\infty, \\ u_c=0.157 \text{ mMU}$$

$$Pf=0, \quad A=173; \quad E_v''=\infty, \\ u_c=0.157 \text{ mMU}, \quad u_s/u_c=94.7$$

appear in the third, fourth, and fifth rows of Table V.

Perhaps the most interesting feature of Table V is the almost constant numerical values in the

seventh and ninth columns; it appears that the symmetry and volume energy coefficients are determined by the empirical energy surface alone without regard to the properties exhibited by nuclear matter under a uniform change of scale.

Figure 2 exhibits the theoretical packing fraction curves computed from the fourth and fifth rows of Table V. The first four rows yield almost identical curves so only one is plotted. It is evident that the uniformity results from (a) fixing the points at which the packing fraction vanishes and (b) adjusting u_c to fit the "Coulomb" energy differences of light odd nuclei. Both branches are extended beyond their respective limits of validity to aid in visualizing the probable interpolation curves. A few experimental points taken from curve (b) of Fig. 1 are included for comparison.

The solid curve (rows 1-4) will be discussed first. On the lower branch the agreement is satisfactory. Ne^{20} and Mg^{24} lie above the theoretical curve, possibly because they occur near

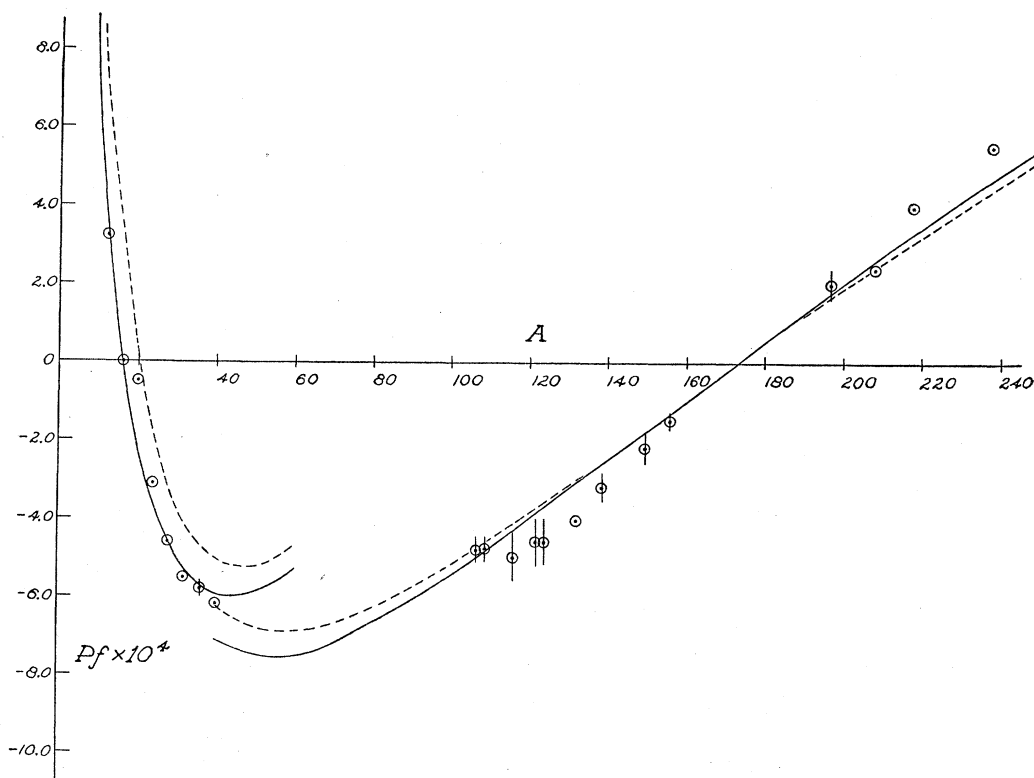


FIG. 2. Theoretical packing fraction curves. Solid curve— $E_v''=\infty$, $u_c=0.157$ mMU; dashed curve— $E_v''=\infty$, $u_c=0.157$ mMU, $u_s/u_c=94.7$; ϕ —experimental points.

the beginning of the shell which closes at Ca⁴⁰. It appears that the notion of surface energy is applicable to very light nuclei of the alpha-particle type (including C¹²) and, moreover, combines satisfactorily with the nuclear radii deduced from the "Coulomb" energy differences of light odd nuclei. On the upper branch the agreement is only fair, and it must be emphasized that the assumption of a finite compressibility coefficient hardly modifies the theoretical curve.

The dashed curve (Bohr-Wheeler value of u_s/u_c) is unsatisfactory on the lower branch and somewhat inferior to the solid curve on the upper branch. A quantitative measure of this inferiority is supplied by the statement that a five percent decrease in r_v applied to the dashed curve brings the upper branch into coincidence with the solid curve.

Equation (31) provides the possibility of reconciling the Bohr-Wheeler value of u_s/u_c with the semi-empirical packing fraction curve. For $E_v'' = 50A$ mMU, $k_s = k_\tau = 0$ and $u_c = 0.161$ mMU

$$u_s/u_c < 94.7[1 - 0.072] = 87.8 \quad (48)$$

while for $E_v'' = 50A$, $k_s = 0.5$, $k_\tau = 0$ and $u_c = 0.169$ mMU

$$u_s/u_c < 94.7[1 - 0.051] = 89.8. \quad (49)$$

The inequalities result from the neglect of the symmetry energy terms in Eq. (31). With $k_\tau = 1$, Eqs. (48) and (49) are replaced by $u_s/u_c = 86.0$ and 88.9, respectively. The first value is in perfect agreement with the packing fraction analysis while the second is still somewhat high. On the whole these numerical trials support the view that a unified self-consistent theory including both the fission phenomenon and the packing fraction curve is possible but requires dropping the fiction of incompressible nuclear matter.

(E) WIGNER TYPE SYMMETRY ENERGY

In the theory developed and tested by Wigner⁴ and Barkas⁵ the symmetry energy can be expressed as

$$u_\tau \frac{(N-Z)^2 + 8q|N-Z|}{A} \quad (50)$$

if the dependence of the energy on the odd-even

TABLE V. Evaluation of the energy coefficients (in mMU).

E_v''	k_s	$u_v - 8.53$						
		u_s/u_c	u_c	u_c/u_τ	u_c	u_τ	u_s	u_o
50A	0.0	86.02	39.64	0.0085	0.161	19.0	13.9	14.9
50A	0.5	85.88	38.76	0.0088	0.169	19.2	14.5	15.1
30A	0.5	83.12	37.09	0.0094	0.178	19.0	14.8	15.1
∞	\sim	89.56	41.10	0.0081	0.157	19.4	14.1	15.1
∞	\sim	94.7	42.02	0.0081	0.157	19.4	14.8	15.1

properties of N and Z is ignored. The coefficient q is not greater than 1 and may be as small as 0.5.

It is evident that the linear term in $|N-Z|$ tends to prevent the shift of the stability curve away from the straight line $N=Z$. The analytical expression of this statement is embodied in the formula

$$A - 2Z_A = \frac{\gamma A^{5/3}}{1 + \gamma A^{2/3}} \left[1 - \frac{1}{A} - \frac{0.2}{u_c A^{2/3}} - \frac{4q}{\gamma A^{5/3}} \right], \quad (51)$$

derived from the condition $\partial(Pf)/\partial Z = 0$ with omission of the "expansion" term. Equation (51) holds only for positive values of $A - 2Z_A$; the vanishing of the factor in square brackets defines a value of A below which the packing fraction minimum in an isobaric series occurs at $A - 2Z_A \cong 0$. With $u_c = 0.157$, $\gamma = 0.0081$, and $q = 1$, Eq. (51) yields $A = 2Z_A$ at $A = 45$: consequently $A - 2Z_A \cong 0$ holds in the range $A \leq 45$. With $q = \frac{1}{2}$, the critical value of A is 30. Actually deviations from $N=Z$ (in even nuclei) occur below these critical values, but there is no systematic trend away from the straight line until mass number 50 is passed. The deviations find a ready explanation in the complete expression of Wigner's theory.

In the present discussion the analog of Eq. (38) is

$$2\gamma = \frac{A - 2Z_A + 4q}{A^{3/2} Z_A} [1 - X_1 - X_2]^{-1}, \quad (52)$$

which differs from Eq. (38) only in the replacement of $A - 2Z_A$ by the larger quantity $A - 2Z_A + 4q$.

(F) DETAILED STUDY OF THE MASS VERSUS N, Z SURFACE; EVEN-ODD CHARACTERISTICS OF NUCLEAR SYSTEMS

The function Z_A follows the general trend of the empirical distribution of Z against A with

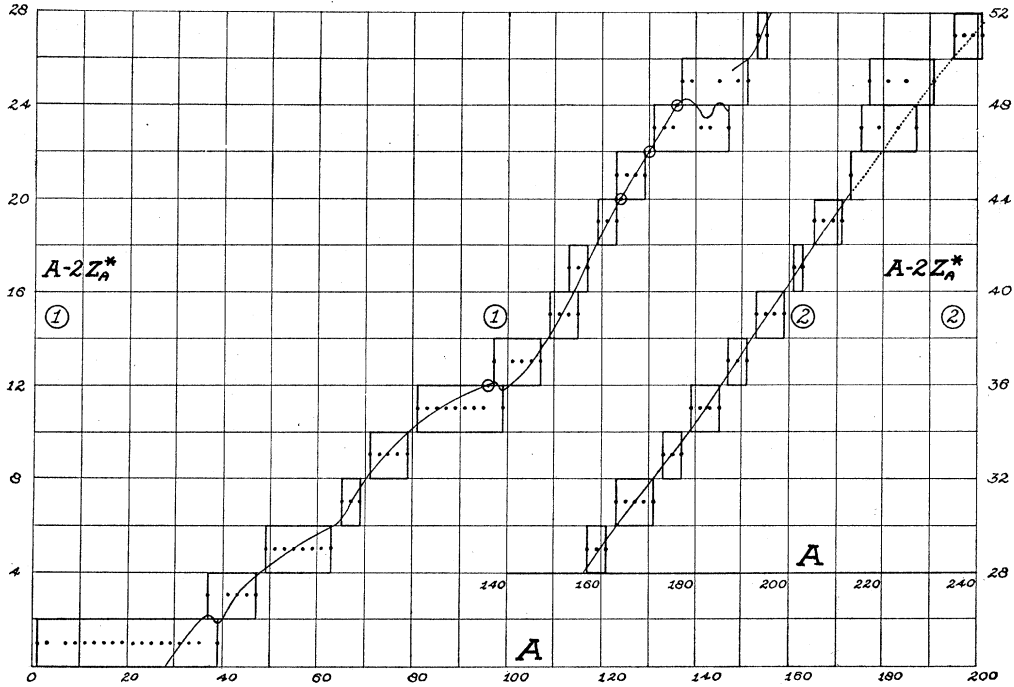


FIG. 3. The mass valley in the $N-Z, A$ plane.

great precision but fails to show the detailed structure. In the present discussion this structure is utilized to compute u_r as a function of mass number. The empirical relation between

TABLE VI. Functions of Z_A^* .

A	Z_A^*	$(A-2Z_A^*)/Z_A^*A^{2/3}$	$10^4\gamma^*$	$4u_c/\gamma^*$	α	$(\gamma^*-\gamma)10^4$
50	22.9	0.0135	77.0	82	90	-4.0
60	27.2	0.0134	75.3	84	94	-5.7
65	29.4	0.0133	74.4	84	94	-6.6
70	31.1	0.0148	82.3	76	87	1.2
75	33.0	0.0153	84.5	74	85	3.5
80	35.0	0.0154	84.6	74	86	3.6
85	37.0	0.0154	84.5	74	86	3.5
90	39.2	0.0147	80.4	78	91	-0.6
95	41.5	0.0139	75.7	83	96	-5.3
100	44.0	0.0127	69.0	91	105	-12.0
105	46.1	0.0127	68.9	91	105	-12.1
110	47.8	0.0131	71.0	88	102	-10.0
115	49.3	0.0140	75.6	83	98	-5.4
120	50.8	0.0149	80.3	78	93	-0.7
125	52.3	0.0156	84.0	75	91	3.0
130	54.0	0.0159	85.5	74	90	4.5
135	55.7	0.0161	86.4	73	89	5.4
140	58.0	0.0154	82.3	76	93	1.3
145	60.4	0.0145	77.5	81	98	-3.5
150	62.1	0.0147	78.5	80	98	-2.5
155	63.7	0.0150	80.0	78	97	-1.0
160	65.4	0.0151	80.4	78	97	-0.6
170	69.2	0.0149	79.4	79	98	-1.6
180	72.8	0.0148	78.6	80	100	-2.4
190	76.3	0.0148	78.5	80	101	-2.5
200	79.8	0.0148	78.3	80	101	-2.7

Z_A and A is determined in large measure by the data for odd nuclei alone.²¹ A convenient plot appears in Fig. 3. The solid curve presumably runs along the bottom of the mass valley as it winds across the $N-Z, A$ plane. To avoid confusion, values of Z taken from this curve are denoted by the symbol Z_A^* .

The vertical extent of the boxes in Fig. 3 fixes upper and lower limits on $A-2Z_A^*$ consistent with the stability of the known odd nuclei. These nuclei appear on the diagram as dots along the horizontal axis of the boxes. Stable isobaric triples occur at mass numbers 96, 124, 130, and 136. The curve is drawn to pass through points determined by the average isotopic number of the stable nuclei at these mass numbers. ${}_{62}\text{Sa}^{148}$ is placed at some distance from the bottom of the mass valley by a discontinuity at mass numbers 147-148. The product nucleus ${}_{60}\text{Nd}^{144}$ resulting from the α -decay of ${}_{62}\text{Sa}^{148}$ then falls directly on the solid curve. There is a strong suggestion that the rare isotope ${}_{64}\text{Ga}^{152}$ may exhibit long-lived alpha-activity. The comparatively low relative abundance of

²¹ G. Gamow, *Atomic Nuclei and Nuclear Transformations* (Oxford University Press, New York, New York, 1937).

the suspected active isotope may be responsible for the failure to observe alpha-activity in gadolinium.

Between mass numbers 210–220 the observed stability-instability relations^{22,23} appear to require separate curves for even and odd nuclei. The dotted portion of the curve is a compromise solution representing the general trend of the mass valley without regard to local irregularities.

The closing of the $2s-3d$ neutron shell at $N=20$ is generally held responsible for the instability of ${}_{18}\text{A}^{39}$ relative to ${}_{19}\text{K}^{39}$. It is interesting that the geometric pattern of stable nuclei shown by Fig. 3 near $A=39$ is repeated at $A=99$. However, the interpretation at the latter point is more difficult, because the nuclei involved are ${}_{43}\text{Tc}^{99}$ (unstable) and ${}_{44}\text{Ru}^{99}$ (stable). This stability-instability relation does not suggest the formation of a closed shell in either nucleus.

Equation (38) with Z_A replaced by Z_A^* serves

to define γ (now denoted by γ^*) as a function of mass number. According to Eq. (41) the mass of a nucleus can be represented in the form

$$M(Z, A) = M(Z_A^*, A) + \alpha[(Z - Z_A^*)^2/A] \quad (53)$$

in the approximation which neglects the even-odd properties of N and Z . Here

$$\alpha = \frac{1}{2}A^2[(\partial^2/\partial Z^2)Pf \times 10^3]_{Z_A^*} \quad (54)$$

can be computed from Eq. (42) with γ replaced by γ^* . This procedure for estimating M and α parallels a closely related discussion by Bohr and Wheeler.¹⁴ The present treatment is potentially more accurate, since it includes the effect of the "expansion" energy. However, the additional term is small. The functions $4u_c/\gamma^*$, α and $(\gamma^* - \gamma) \times 10^4$ listed in Table VI have been computed under the conditions holding in the fourth row of Table V ($E_v'' = \infty$, $u_c = 0.157$ mMU).

As Fig. 2 makes evident, the packing fraction curves associated with constant values of γ are

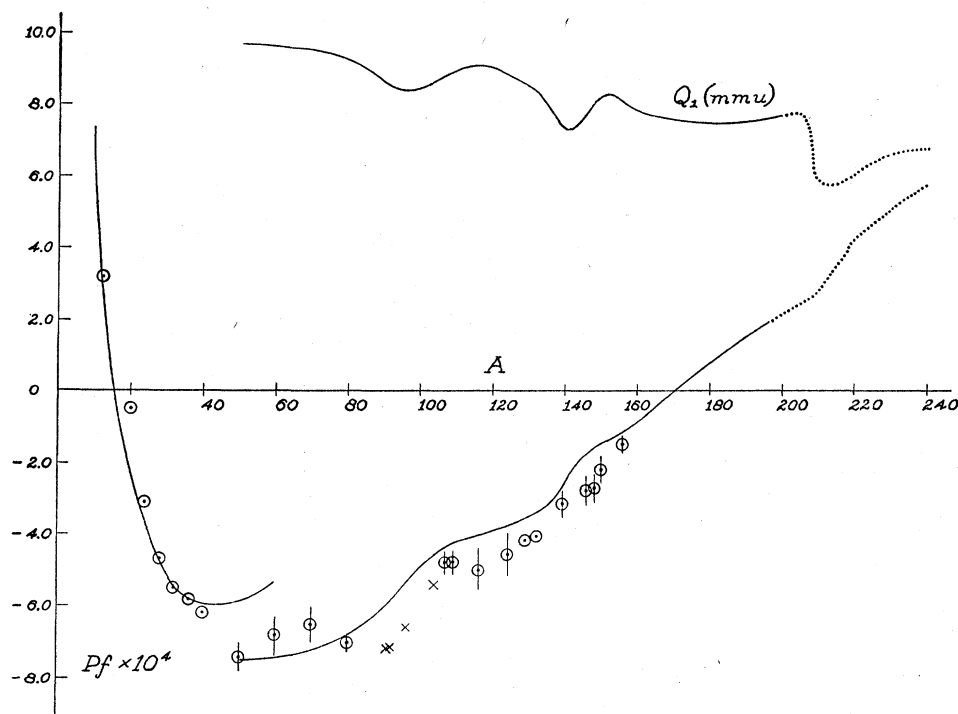


FIG. 4. The theoretical packing fraction curve corrected for the oscillatory variation of the symmetry energy coefficient with mass number. The dotted portion is taken directly from the experimental points. Included is a theoretical curve (Q_1) giving the mean excitation energy produced by the capture of a slow neutron.

²² G. T. Seaborg, Rev. Mod. Phys. 16, 1 (1944).

²³ E. Segrè, unclassified charts compiled for the Manhattan Project (July, 1946).

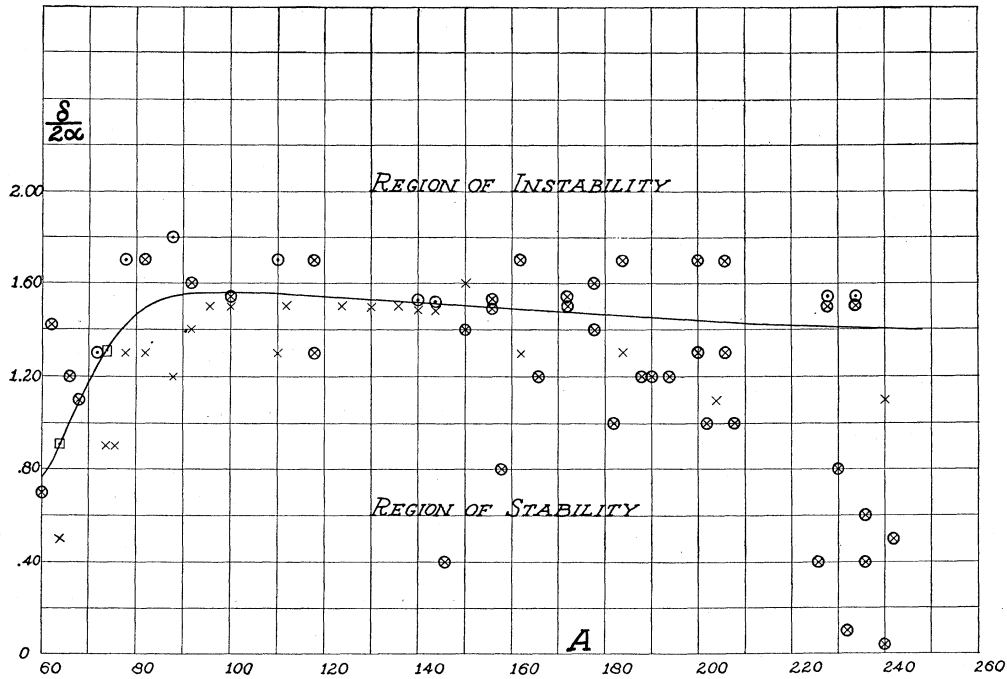


FIG. 5. The location of the stability limit for even-even nuclei.

- × - stable
- - unstable
- ⊕ - unknown

very nearly straight lines above mass number 80. This behavior may be associated with the smooth variation of Z_A with A . Empirically Z_A^* is not a smooth function of A (since γ^* is oscillatory), and the packing fraction curve is decidedly not straight above mass number 80. These two failures to conform to the simple theory can be correlated in a simple manner by inserting the function $\gamma^*(A)$ into Eq. (44) in place of γ . The resulting packing fraction formula can be expressed as

$$\left[\frac{Pf \times 10^3}{u_c} \right]_{\gamma^*} = \left[\frac{Pf \times 10^3}{u_c} \right]_{\gamma} + \frac{\Delta Pf \times 10^3}{u_c},$$

$$\frac{\Delta Pf \times 10^3}{u_c} \cong (\gamma - \gamma^*) \quad (55)$$

$$\times \left[\left(\frac{A^{\frac{2}{3}}}{1 + \gamma A^{\frac{2}{3}}} \right)^2 - 2.5 \frac{A^{\frac{2}{3}}}{1 + \gamma A^{\frac{2}{3}}} \right].$$

Figure 4 reveals the extent of the improved agreement. A number of points taken from

curve b of Fig. 1 are included to facilitate comparison with experimental results.

Bohr and Wheeler adapt Eq. (53) to the dependence of M on the even-odd properties of N and Z by the substitutions:

$$\begin{aligned} \alpha(Z - Z_A^*)^2 &\rightarrow \alpha(Z - Z_A^*)^2 + \frac{1}{2}\delta, & Z \text{ odd, } N \text{ odd,} \\ &\rightarrow \alpha(Z - Z_A^*)^2 - \frac{1}{2}\delta, & Z \text{ even, } N \text{ even,} \\ &\rightarrow \alpha(Z - Z_A^*)^2, & A \text{ odd.} \end{aligned} \quad (56)$$

Equation (56) implies the following replacement in Eq. (2):

$$\begin{aligned} u_r(N - Z)^2 &\rightarrow u_r(N - Z)^2 + \frac{1}{2}\delta, & Z \text{ odd, } N \text{ odd,} \\ &\rightarrow u_r(N - Z)^2 - \frac{1}{2}\delta, & Z \text{ even, } N \text{ even,} \\ &\rightarrow u_r(N - Z)^2, & A \text{ odd.} \end{aligned} \quad (57)$$

In an isobaric series of even-even nuclei the inequality

$$\delta/2\alpha > |Z - Z_A^*| - \frac{1}{2} \quad (58)$$

holds for the stable members of the series, while the reversed inequality holds for the unstable

members.¹⁴ Here instability means that energy is available for the emission of a negative electron or for the absorption of an electron (*K*-capture). Figure 5 shows a plot of the right-hand member of Eq. (58) for those stable, unstable, and unknown even nuclei which border closely on the stability limit. An uncertainty of at least ± 0.2 must be associated with all points because of the uncertainty in the determination of Z_A^* . Crosses and circles denote known²²⁻²⁴ stable and unstable nuclei respectively; where the nucleus is unknown the point is indicated by a cross within a circle.

The solid line for $\delta/2\alpha$ as drawn in Fig. 5 does not permit stable isobaric triples above mass number 150. In this range the limit of stability allows only stable doubles and singles. Since triples and singles presumably occur only when Z_A^* falls sufficiently close to an even integer, one expects about the same number of stable singles above $A = 150$ as stable triples below.

The unknown nuclei below and near the stability limit may be grouped into two classes:

*Stability indicated with respect to β^\pm emission or *K*-capture.*

${}_{62}\text{Sm}^{146}$, ${}_{66}\text{Dy}^{158}$, ${}_{72}\text{Hf}^{182}$, ${}_{82}\text{Pb}^{202}$, ${}_{84}\text{Po}^{208}$, ${}_{90}\text{Th}^{226}$,
 ${}_{92}\text{U}^{230}$, ${}_{92}\text{U}^{232}$, ${}_{92}\text{U}^{236}$, ${}_{94}\text{Pu}^{236}$, ${}_{94}\text{Pu}^{240}$, ${}_{94}\text{Pu}^{242}$.

$$\left. \begin{aligned} \Delta E^{(-)} &= (2\alpha/A)(Z_A^* - Z^{(-)} - \frac{1}{2}) \\ \Delta E^{(k)} &= (2\alpha/A)(Z^{(+)} - Z_A^* - \frac{1}{2}) \\ \Delta E^{(+)} &= \Delta E^{(k)} - 2mc^2. \end{aligned} \right\} \begin{aligned} &+ 0 \quad (A \text{ odd}), \\ &- \delta/A \quad (Z^{(\pm)} \text{ even}, A \text{ even}), \\ &+ \delta/A \quad (Z^{(\pm)} \text{ odd}, A \text{ even}), \end{aligned} \quad (59)$$

There exist nuclei, of even mass number, capable of both β^+ and β^- transitions. For these

$$\begin{aligned} \Delta E^{(-)} + \Delta E^{(k)} &= 2/A \cdot (\delta - \alpha), \\ \Delta E^{(-)} - \Delta E^{(k)} &= 4\alpha/A \cdot (Z_A^* - Z). \end{aligned} \quad (60)$$

Examples illustrating the application of Eq. (60) appear in Table VII. Energies, expressed in mMU, are taken from references 22 and 23. A radiation transition of 0.62 mMU occurs in the arsenic reaction resulting in an ambiguity in the assignment of energies to the positive and negative branches. Figure 3 favors the association of the gamma-quantum with the positive branch. The computed values of $\delta/2\alpha$ appear in Fig. 3 as squares, and the curve is drawn to

Stability uncertain.

${}_{46}\text{Pd}^{100}$, ${}_{52}\text{Te}^{118}$, ${}_{62}\text{Sm}^{156}$, ${}_{66}\text{Dy}^{156}$, ${}_{66}\text{Dy}^{166}$, ${}_{68}\text{Er}^{172}$,
 ${}_{72}\text{Hf}^{172}$, ${}_{74}\text{W}^{178}$, ${}_{74}\text{W}^{188}$, ${}_{78}\text{Pt}^{190}$, ${}_{76}\text{Os}^{194}$, ${}_{78}\text{Pt}^{200}$, ${}_{84}\text{Po}^{206}$,
 ${}_{86}\text{Rn}^{212}$, ${}_{86}\text{Rn}^{214}$, ${}_{86}\text{Rn}^{216}$, ${}_{86}\text{Rn}^{218}$, ${}_{88}\text{Ra}^{222}$.

The stability of ${}_{46}\text{Pd}^{100}$ would fit neatly into the pattern of Fig. 3 by completing a stable triple at $A = 100$ to balance one known to exist at $A = 96$.

Note added in proof: The \oplus at $A = 158$ in Fig. 5 should be replaced by \times since it refers to ${}_{66}\text{Dy}^{158}$ which is a known stable nucleus. J. J. Howland, D. H. Templeton, and I. Perlman, Phys. Rev. **71**, 552 (1947) report that Po^{206} is unstable (both *K* capture and α -emission is observed) while Po^{208} is apparently stable (only α -emission is observed). These observations confirm the assignment of ${}_{84}\text{Po}^{208}$ to the stable class. Thus the \oplus at $A = 208$ in Fig. 5 can now be replaced by \times ; also the upper \oplus at $A = 206$ should be replaced by \circ .

L. A. Turner, Rev. Mod. Phys. **291**, 17 (1945), considers the properties of missing heavy nuclei. Turner's conclusions, listed in Table II of the reference, are consistent with the present location of the mass valley (dotted portion of the curve in Fig. 3) and the determination of $\delta/2\alpha$ (Fig. 5) except for ${}_{94}\text{Pu}^{236}$ which is probably a positron emitter according to Turner and probably stable according to the present paper.

Equation (56) determines the energy available for β^\pm transitions between the ground states of initial and product nuclei. The required formulae are

pass through them. An additional example is provided by As^{76} , but $\Delta E^{(-)} + \Delta E^{(+)}$ is too large (~ 5.7 mMU) to fit reasonably into the present analysis.

For even radioactive isobars separated by a stable nucleus Eq. (59) yields

$$\begin{aligned} \Delta E^{(-)} + \Delta E^{(k)} &= 2/A \cdot (\alpha + \delta), \\ \Delta E^{(-)} - \Delta E^{(k)} &= 4\alpha/A \cdot (Z_A^* - Z^{(-)} - 1). \end{aligned} \quad (61)$$

The available experimental material does not

TABLE VII. Analysis of branching β^\pm transitions.

Element	A	Z	$\Delta E^{(-)}$	$\Delta E^{(+)}$	α (Table 6)	$\delta/2\alpha$	Z_A^* (Eq. 60)	Z_A^* (Fig. 3)
Cu	64	29	0.62	0.71	95	0.91	28.8	29.0
As	74	33	1.40	1.59	85	1.39	32.7	32.5
As	74	33	2.02	0.97	85	1.39	33.0	32.5

²⁴ J. M. Siegel, J. Am. Chem. Soc. **68**, 2411 (1946).

conform to the general pattern prescribed by Eq. (61). Possibly the theory is quite inadequate; however, it is also possible that future changes in the assignment of activities and the measurement of energies may improve the agreement.

Many radioactive transitions are known in the A classification²²⁻²⁴ (element and isotope assignment considered certain). The results of a detailed comparison of measured and computed values of $\Delta E^{(\pm)}$ for transitions in the A classification can be summarized as follows:

β^- , $A(\text{odd}) \geq 35$, $A(\text{even}) \geq 60$.

120 examples; of these 25 percent yield discrepancies $|\Delta E^{(\rightarrow)}(\text{observed}) - \Delta E^{(\rightarrow)}(\text{computed})| \geq 1.0$ mMU with the mean discrepancy 1.8 mMU. For the remaining 75 percent the mean value of the discrepancy is ~ 0.4 mMU.

β^+ , $A(\text{odd}) \geq 41$, $A(\text{even}) \geq 56$.

20 examples; 10 show large discrepancies.

In evaluating the apparently unsatisfactory showing of the theory one must remember that Z_A^* is uncertain by at least ± 0.1 resulting in errors in the computed energies ranging from 0.1 mMU ($A \sim 200$) to 0.4 mMU ($A \sim 50$). Also there are no theoretical grounds for excluding small random variations in the packing fraction within an isobaric series. These two sources of error are adequate to account for a mean discrepancy of 0.4 mMU, but leave unexplained the larger discrepancies (mean ~ 1.8 mMU) associated with many radioactive nuclei in the A classification.

Note added in proof: In this connection the history of the 2.6 hr period of nickel is suggestive. Formerly the period was associated with Ni^{68} (classified A) resulting in a large discrepancy between observed and computed disintegration energies. The recent assignment to Ni^{66} (by J. A. Swartout, G. E. Boyd, A. E. Cameron, C. P. Keim, C. E. Larson, Phys. Rev. **70**, 232 (1946)) removes the discrepancy.

(G) THE EXCITATION ENERGY OF INTERMEDIATE SYSTEMS FORMED BY NEUTRON CAPTURE

The intermediate system formed when a nucleus captures a slow neutron begins its life with the excitation energy

$$Q = 10^3[M(Z, A) + n - M(Z, A + 1)]. \quad (62)$$

To facilitate numerical evaluation Q is expressed

as a sum of three terms Q_1 , Q_2 , and Q_3 defined as follows:

$$Q_1 = 10^3[A(1 + Pf_A) - (A + 1)(1 + Pf_{A+1}) + 1.00892] \\ \cong 8.92 - Pf \times 10^3 - A \frac{d}{dA} Pf \times 10^3, \quad (62a)$$

$$Q_2 = \frac{\alpha_A(Z - Z_A^*)^2}{A} - \frac{\alpha_{A+1}(Z - Z_{A+1}^*)^2}{A + 1} \\ \cong 2\alpha/A(Z_{A+1}^* - Z_A^*)(Z - \frac{1}{2}(Z_A^* + Z_{A+1}^*)) \sim 80/A(Z - Z_{A+1}^*), \quad (62b)$$

$$Q_3 = -\delta/2A \quad (Z \text{ even}, A \text{ even}; Z \text{ odd}, A \text{ odd}), \\ = \delta/2A \quad (Z \text{ even}, A \text{ odd}; Z \text{ odd}, A \text{ even}). \quad (62c)$$

A plot of Q_1 , computed from the theoretical packing fraction curve shown on the same diagram, appears in Fig. 4.

The stability of the target nucleus implies $|Z - Z_A^*| \leq \frac{1}{2}$ (A odd) or $|Z - Z_A^*| \leq 2$ (A even), the second inequality following from Eq. (58) with $\delta/2\alpha \sim 1.5$. With $Z_{A+1}^* \sim Z_A^* + 0.2$

$$-56/A \leq Q_2 \leq 24/A \quad (A \text{ odd}), \\ -176/A \leq Q_2 \leq 144/A \quad (A \text{ even}). \quad (63)$$

Because of the numerical relation $\delta \sim 3 \alpha \sim 300$ mMU, $Q_2 - \delta/2A$ is never positive and approaches zero only for those even nuclei quite near the stability limit. Consequently

$$Q \leq Q_1 \quad (Z \text{ even}, A \text{ even}), \\ Q > Q_1 \quad (Z \text{ even}, A \text{ odd}), \\ Q < Q_1 \quad (Z \text{ odd}, A \text{ odd}). \quad (64)$$

The statistical theory of nuclear level density² makes the spacing of levels at the excitation energy Q an exponentially decreasing function of $(Q/\Delta\epsilon)^{\frac{1}{2}}$ ($\Delta\epsilon$ is essentially a unit of excitation energy). The characteristic dependence of Q on the even-odd properties of Z and A should therefore influence the distribution of large capture cross sections among the different nuclear types. However there also exists a specific dependence of level spacing on the even-odd properties of Z and A comparable with the implicit dependence through Q and in the opposite direction.²⁵ Under

²⁵ J. Bardeen and E. Feenberg, Phys. Rev. **54**, 809 (1938).

the tentative hypothesis that the dependence through Q is the larger of the two effects, Eq. (64) yields the rule that odd nuclei with even charge are favored to possess large capture cross sections. The empirical evidence suggests rather an absence of dependence on the even-odd character of Z except for the very largest cross sections which conform to the rule.

Note added in proof: M. J. Inghram, D. C. Hess, Jr., and R. J. Hayden, Phys. Rev. **71**, 561 (1947) have determined the cross sections for slow neutron capture by the separated isotopes of Hg. Large cross sections are found for $A=196$, 199 and small cross sections for $A=200$, 202, 204, 201. These results conform to the pattern suggested by the rule.

It is perhaps significant that a fair proportion of the elements with large capture cross sections occur near the peaks of the Q_1 curve. The first peak centered at $A=115$ is associated with Rh, Ag, Cd, and In, while the second centered at $A=151$ covers the rare earth elements Sm, Eu, Gd, Dy, and Ho.

The function Q_1 appears again in the semi-empirical formula for the energy released in α -decay:

$$Q' = 10^3 [M(Z+1, A+2) - {}_2\text{He}^4 - M(Z-1, A-2)] \\ = Q_1' + Q_2', \quad (65)$$

$$Q_1' = 4 [Pf \times 10^3 + A(\partial/\partial A)Pf \times 10^3 - 1] \text{ mMU} \\ = 4(7.93 - Q_1), \quad (65a)$$

$$Q_2' = (\alpha_{A+2}/A+2)(Z+1 - Z_{A+2}^*)^2 \\ - (\alpha_{A-2}/A-2)(Z-1 - Z_{A-2}^*)^2 \\ \sim (2\alpha/A)(Z_{A-2}^* + 2 - Z_{A+2}^*)(Z - Z_A^*). \quad (65b)$$

(H) THE SYMMETRY QUANTUM NUMBERS $PP'P''$

Consider a gas of non-interacting neutrons and protons confined to the volume

$$(4\pi/3)R^3 = (4\pi/3)r_0^3 A.$$

In accordance with Wigner's notation, the integers $\Lambda_1, \Lambda_2, \Lambda_3, \Lambda_4$ refer, in the order named, to the number of

- (1) neutrons with positive spin
- (2) neutrons with negative spin
- (3) protons with positive spin
- (4) protons with negative spin

In the present calculation¹³ each type of particle forms a completely degenerate gas. Surface

effects and the detailed structure of the single particle levels are ignored. The quantization of the single particle motion and the complete degeneracy of the gas are expressed in the statement that momentum space is fully occupied up to a maximum momentum P_{im} determined by the relation

$$\Lambda_i h^3 = (4\pi/3)^2 (P_{im} R)^3. \quad (66)$$

Equation (66) equates the number of occupied cells in phase space, each of volume h^3 , to the product of the configuration and momentum space volumes.

Maximum and average kinetic energies, ϵ_{im} and $\bar{\epsilon}_i$, are defined by the equations

$$\epsilon_{im} = \frac{1}{2M} P_{im}^2 = \frac{h^2}{2MR^2} \left(\frac{3}{4\pi}\right)^{4/3} \Lambda_i^{2/3}, \quad (67) \\ \bar{\epsilon}_i = \frac{1}{2M} \int_0^{P_{im}} p^4 dp / \int_0^{P_{im}} p^2 dp = \frac{3}{5} \epsilon_{im}.$$

The total kinetic energy of gas i is then simply $T_i = \Lambda_i \bar{\epsilon}_i$. For the complete system

$$T = \sum \Lambda_i \bar{\epsilon}_i = \frac{3h^2}{10MR^2} \left(\frac{3}{4\pi}\right)^{4/3} \sum \Lambda_i^{5/3}. \quad (68)$$

The behavior of the kinetic energy in an isobaric series can be studied by allowing the separate Λ 's to vary while the sum remains

TABLE VIII.

Structure symbol	$A=4k$				W
	P	P'	P''	W_1	
$3^0 2^0 1^0$	0	0	0	0	0
31	1	1	0	2	8
22	2	0	0	4	12
$32^2 1$	3	1	0	10	24
2^4	4	0	0	16	32
$32^4 1$	5	1	0	26	48
2^6	6	0	0	36	60

TABLE IX.

Structure symbol	$A=4k+2$				W_2
	P	P'	P''	W_1	
2	1	0	0	1	5
321	2	1	0	5	15
2^3	3	0	0	9	21
$32^3 1$	4	1	0	17	35
2^5	5	0	0	25	45
$32^5 1$	6	1	0	37	63
2^7	7	0	0	49	77

TABLE X.

Structure symbol	$A = 4k + 1$			W_1	W_2
	P	P'	P''		
1	1/2	1/2	1/2	3/4	15/4
32	3/2	1/2	-1/2	11/4	39/4
2 ² 1	5/2	1/2	1/2	27/4	71/4
32 ³	7/2	1/2	-1/2	51/4	111/4
2 ⁴ 1	9/2	1/2	1/2	83/4	159/4
32 ⁵	11/2	1/2	-1/2	123/4	215/4
2 ⁶ 1	13/2	1/2	1/2	171/4	279/4

constant. To make this behavior explicit let

$$\begin{aligned} P &= \frac{1}{2}(\Lambda_1 + \Lambda_2 - \Lambda_3 - \Lambda_4) = \frac{1}{2}(N - Z), \\ P' &= \frac{1}{2}(\Lambda_1 - \Lambda_2 + \Lambda_3 - \Lambda_4) = S_+ - S_-, \\ P'' &= \frac{1}{2}(\Lambda_1 - \Lambda_2 - \Lambda_3 + \Lambda_4). \end{aligned} \quad (69)$$

These are the quantum numbers introduced by Wigner to describe the symmetry properties of nuclear systems.⁴ In terms of the P 's¹³

$$T = \frac{27}{40} \left(\frac{\pi}{3} \right)^{2/3} \frac{\hbar^2 A^{5/3}}{MR^2} \times \left[1 + \frac{20}{9} \frac{P^2 + P'^2 + P''^2}{A^2} + \dots \right]. \quad (70)$$

For

$$r_v = r_0 \equiv 1.47 \times 10^{-13} \text{ cm},$$

$$T = 14.4A \left[1 + \frac{20}{9} \frac{P^2 + P'^2 + P''^2}{A^2} + \dots \right] \text{ mMU}. \quad (71)$$

The quantum members $PP'P''$ have been introduced here in an extremely restricted sense. There is no need to restate the general definition, but one important property can be pointed out. A brief examination of a diagram showing the fourfold system of single particle levels clearly indicates that a given set of numbers $PP'P''$ can be associated with all nuclei for which $-2P \leq N - Z \leq 2P$. Thus all isobaric nuclei in the range $-2P \leq N - Z \leq 2P$ possess states to which Eq. (70) applies.

The spacing $\Delta\epsilon$ of the single particle levels at the top of the occupied region can be derived from Eqs. (68) or (70). For simplicity suppose $\Lambda_i = \Lambda = A/4$. Then

$$\begin{aligned} \Delta\epsilon &= \frac{1}{2} [T(\Lambda + 1, \Lambda + 1, \Lambda - 1, \Lambda - 1) \\ &\quad - T(\Lambda, \Lambda, \Lambda, \Lambda)] \\ &= 40T/9A^2 \cong 64/A \cdot (r_0/r_v)^2 \text{ mMU}. \end{aligned} \quad (72)$$

Equation (72) has the virtue of suggesting a procedure for computing an "effective" single particle level spacing in actual nuclei. The obvious generalization is

$$\begin{aligned} \Delta\epsilon_{\text{eff}} &= \frac{1}{2} [E_r(\Lambda + 1, \Lambda + 1, \Lambda - 1, \Lambda - 1) \\ &\quad - E_r(\Lambda, \Lambda, \Lambda, \Lambda)], \\ &= \frac{8u_r}{A} \sim \frac{154}{A} \text{ mMU}. \end{aligned} \quad (73)$$

The numerical coefficient is taken from Table V. A possible application of Eq. (73) occurs in the statistical theory of level density. It is known that the statistical theory,² with $\Delta\epsilon$ for the single particle level spacing, greatly underestimates the average spacing of the nuclear levels as a function of excitation energy. In view of the fact that

$$\Delta\epsilon_{\text{eff}} \sim 2.4\Delta\epsilon(r_v/r_0)^2, \quad (74)$$

the substitution of $\Delta\epsilon_{\text{eff}}$ for $\Delta\epsilon$ in the statistical theory produces a greatly reduced level density and a somewhat closer correspondence with the observations.

In this connection Bardeen²⁶ has computed the single particle level spacing $\Delta\epsilon_B$ for a specific model of nuclear forces having the essential saturation property. His results, based on the statistical approximation, may be summarized in the relation $\Delta\epsilon_B \sim 2\Delta\epsilon$.

The appearance of the "symmetry" function

$$W_1(PP'P'') = P^2 + P'^2 + P''^2 \quad (75)$$

in Eq. (70) suggests replacing the symmetry energy in Eq. (1) by

$$4u_r(W_1/A). \quad (76)$$

Actually the modified symmetry energy of Eq. (76) does represent an improvement since it can be related to the observed even-odd characteristics of nuclei.

Wigner's analysis of the nuclear symmetry problem⁴ yields the symmetry function.

$$W_2(PP'P'') = P^2 + P'^2 + P''^2 + 4P + 2P' \quad (77)$$

on the basis of fairly general assumptions concerning the symmetry properties of the nuclear Hamiltonian and the nature of the interaction

²⁶ J. Bardeen, Phys. Rev. **51**, 799 (1937).

between pairs of particles. In the detailed comparison with experiment Wigner uses a linear combination of W_1 and W_2 with the coefficient of W_1 taken from the statistical theory of the kinetic energy and the coefficient of W_2 adjusted to fit the empirical stability-instability relations. As explained in Section (E) the correlation with experiment begins to break down just where the systematic trend away from equal numbers of neutrons and protons is getting started.

Tables VIII–X list numerical values of W_1 and W_2 for completely degenerate systems. The structure symbol shows the number of triply, doubly and singly occupied levels in terms of the single particle model or the irreducible representation of the symmetric group to which the state in question belongs from the more general point of view adopted by Wigner. To adapt Table X to nuclei of the type $4k+3$, replace “1” by “3” and “3” by “1” in the structure symbols and reverse the sign of P'' .

General relations between successive lines of the tables are easily inferred and can be used to prove the relations

$$\begin{aligned} W_1 - \frac{1}{2} &= P^2 - \frac{1}{2}, N, Z \text{ even,} \\ &= P^2 + \frac{1}{2}, N, Z \text{ odd,} \\ &= P^2, A \text{ odd.} \end{aligned} \quad (78)$$

$$\begin{aligned} W_2 - \frac{3}{2} &= P^2 + 4P - \frac{3}{2}, N, Z \text{ even,} \\ &= P^2 + 4P + \frac{3}{2}, N, Z \text{ odd,} \\ &= P^2 + 4P, A \text{ odd.} \end{aligned} \quad (79)$$

According to Eq. (78) or (79) the masses of isobaric even nuclei fall on two parabolic curves; one (the lower) for even N and Z , the other (the upper) for odd N and Z . The vertical separation of the parabolas is

$$4u_\tau/A, \text{ Eq. (78)} \quad (80)$$

or

$$12u_\tau/A, \text{ Eq. (79).}$$

Empirically, above mass number 80, the spacing δ/A (from Eq. (56)) is very nearly $15u_\tau/A$ or about double the value given by Wigner's linear combination of W_1 and W_2 .

Two theorems on isobaric stability will now be derived from the general symmetry function

$$\begin{aligned} W_3 &= P^2 + 4qP - t/2, N, Z \text{ even,} \\ &= P^2 + 4qP + t/2, N, Z \text{ odd,} \\ &= P^2 + 4qP, A \text{ odd.} \end{aligned} \quad (81)$$

In discussing Eq. (81) it proves convenient to use language appropriate to the three (Wigner) diagrams, (Fig. 6), which illustrate the symmetry dependence of the nuclear energy for a special form of $W_3(q=0, t=3)$. The lines connecting isobaric nuclei in states with the same $PP'P''$ are drawn horizontal, but in reality slope down to the right because of the variation in Coulomb energy along an isobaric series. The neutron-hydrogen mass difference tends to produce a positive slope, but the effect is too small to overcome the opposite tendency produced by the Coulomb energy. All lines in one diagram have the same slope at the vertical axis. Moreover the curvature is negligible (subject to the restriction $P \ll A$); hence all lines in one diagram are substantially parallel. Finally the slope is a monotonic increasing function of A .

Theorem 1

Subject to the condition $t > 1$, Eq. (81) makes all odd-odd nuclei unstable. The proof follows

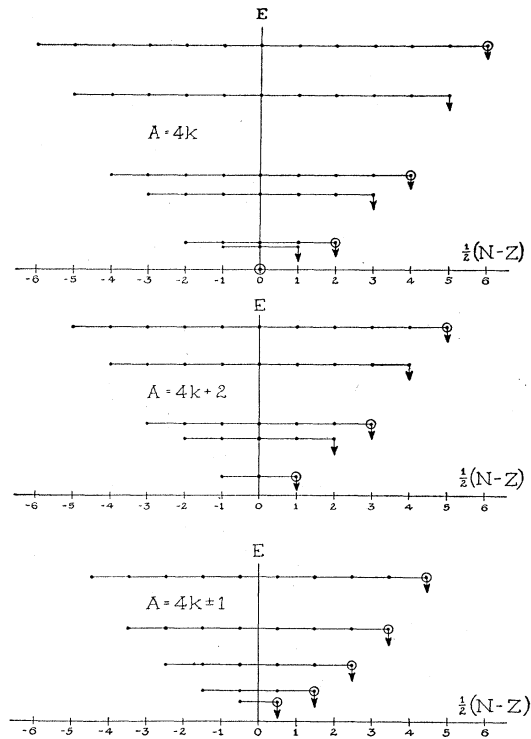


FIG. 6. Wigner type energy diagrams.

TABLE XI. Theoretical and observed correlations in isotopic number.

$N-Z$		Mass numbers for first occurrence of stated $N-Z$	
Odd A	Even A	Odd A	Even A
3	4	37	36
5	6	49	46
7	8	65	64
9	10	71	70
11	12	81	76
13	14	87(?)	86
15	16	109	96
17	18	113	110
19	20	119	116
21	22	123	122
23	24	131	124
25	26	137	130
27	28	153	136
29	30	157	150
31	32	163	160
33	34	173	170
35	36	179	176
37	38	187	186
39	40	193	192
41	42	201	198
43	44	205	204
45	46	213	214
47	48	215	216(?) 220
49	50	217	218(?) 222
51	52	235	232
53	54	unknown	238

immediately from the inequality

$$P^2 + 4qP + t/2 - \{(P-1)^2 + 4q(P-1) - t/2\} > (P+1)^2 + 4q(P+1) - t/2 - \{P^2 + 4qP + t/2\}, \quad (82)$$

which reduces to $t > 1$. Equation (82) states that $N-Z=2(P+1)$ (even, even) falls below $N-Z=2P$ (odd, odd) before the latter point falls below $N-Z=2(P-1)$ (even, even).

The exceptions H^2 , Li^6 , B^{10} , and N^{14} are understood in terms of a spin dependent nuclear force. Beyond $A=14$, the Coulomb energy is large enough to overcome the disturbing influence of the spin dependent force, and the theoretical pattern agrees with the observations.

Theorem 2

The shift from $P-1$ stable to $P+1$ stable in the even-even series occurs at the same slope (and hence at nearly the same mass number) as the corresponding shift from $P-\frac{1}{2}$ stable to $P+\frac{1}{2}$ stable in the nuclei of odd mass number.

The theorem expresses the physical meaning of the identity:

$$(P+1)^2 + 4q(P+1) - t/2 - \{(P-1)^2 + 4q(P-1) - t/2\} = 2[(P+\frac{1}{2})^2 + 4q(P+\frac{1}{2}) - \{(P-\frac{1}{2})^2 + 4q(P-\frac{1}{2})\}]. \quad (83)$$

In terms of $N-Z$ the theorem states that nuclei with

$$N-Z = 2n-1 \quad (A \text{ odd}), \\ N-Z = 2n \quad (A \text{ even}),$$

first become stable at nearly the same mass number.

Numerical results are listed in Table XI. Alpha-emitters are included since the stability argument refers to stability within an isobaric series. The table shows

- 17 good correlations, $A_{\text{odd}} - A_{\text{even}} \leq 3$,
- 3 near misses, $A_{\text{odd}} - A_{\text{even}} = 5$
- 3 poor correlations, $A_{\text{odd}} - A_{\text{even}} = 7$,
- 2 extreme failures, $A_{\text{odd}} - A_{\text{even}} = 13, 17$.

There is also one point for which no odd representative is known. The energies available in the radioactive transitions starting from ${}_{36}\text{Kr}^{85}$, ${}_{37}\text{Rb}^{87}$, and ${}_{38}\text{Sr}^{89}$ are 0.85, 0.3, and 1.5–1.3 Mev in the order named. Thus ${}_{37}\text{Rb}^{87}$ barely misses being stable and consequently may be counted as supporting the theory. The same statement might also be applied to ${}_{84}\text{Po}^{216}$ and ${}_{84}\text{Po}^{218}$.

The possibility cannot be completely excluded that rare isotopes required to eliminate one or more of the exceptional cases actually are stable but exist in such small abundance as to have so far escaped detection. However, a survey of the known stable and instable nuclei in regions where the exceptions occur leads to the tentative conclusion that the exceptional cases are all real. Wigner²⁷ has remarked that the extreme failures ($A=109, 153$) are followed in the table by nuclei with large capture cross sections for slow neutrons.

Theorem 2 is not new,²⁸ but the present discussion has the advantage of generality in that no restrictions are placed on q and t except that required to avoid the stability of odd-odd nuclei. Consequently the theorem is applicable over the whole range of nuclear species.

²⁷ Private communication.

²⁸ E. Wigner, Phys. Rev. 51, 106 (1937).